INTERFACE

rsif.royalsocietypublishing.org

Research

**Cite this article:** Watson GS, Cribb BW, Schwarzkopf L, Watson JA. 2015 Contaminant adhesion (aerial/ground biofouling) on the skin of a gecko. *J. R. Soc. Interface* **12**: 20150318. http://dx.doi.org/10.1098/rsif.2015.0318

Received: 10 April 2015
Accepted: 18 May 2015

**Subject Areas:**
biomaterials

**Keywords:**
gecko, contamination, lizard, adhesion, biofouling, pollen

**Authors for correspondence:**
Gregory S. Watson
e-mail: gwatson1@usc.edu.au
Jolanta A. Watson
e-mail: jolanta.watson@griffith.edu.au

Electronic supplementary material is available at http://dx.doi.org/10.1098/rsif.2015.0318 or via http://rsif.royalsocietypublishing.org.

THE ROYAL SOCIETY PUBLISHING

# Contaminant adhesion (aerial/ground biofouling) on the skin of a gecko

Gregory S. Watson[1], Bronwen W. Cribb[2], Lin Schwarzkopf[3] and Jolanta A. Watson[1]

[1]School of Science and Engineering, Faculty of Science, Health, Education and Engineering, University of the Sunshine Coast, Maroochydore DC, Queensland 4558, Australia
[2]Centre for Microscopy and Microanalysis and School of Biological Sciences, The University of Queensland, St Lucia, Queensland 4072, Australia
[3]School of Marine and Tropical Biology, James Cook University, Townsville, Queensland 4811, Australia

GSW, 0000-0001-9843-9211; BWC, 0000-0002-6309-1400; LS, 0000-0002-1009-670X; JAW, 0000-0002-5027-9025

In this study, we have investigated the micro- and nano-structuring and contaminant adhesional forces of the outer skin layer of the ground dwelling gecko—*Lucasium steindachneri*. The lizard's skin displayed a high density of hairs with lengths up to 4 µm which were spherically capped with a radius of curvature typically less than 30 nm. The adhesion of artificial hydrophilic (silica) and hydrophobic ($C_{18}$) spherical particles and natural pollen grains were measured by atomic force microscopy and demonstrated extremely low values comparable to those recorded on superhydrophobic insects. The lizard scales which exhibited a three-tier hierarchical architecture demonstrated higher adhesion than the trough regions between scales. The two-tier roughness of the troughs comprising folding of the skin (wrinkling) limits the number of contacting hairs with particles of the dimensions used in our study. The gecko skin architecture on both the dorsal and trough regions demonstrates an optimized topography for minimizing solid–solid and solid–liquid particle contact area, as well as facilitating a variety of particulate removal mechanisms including water-assisted processes. These contrasting skin topographies may also be optimized for other functions such as increased structural integrity, levels of wear protection and flexibility of skin for movement and growth. While single hair adhesion is low, contributions of many thousands of individual hairs (especially on the abdominal scale surface and if deformation occurs) may potentially aid in providing additional adhesional capabilities (sticking ability) for some gecko species when interacting with environmental substrates such as rocks, foliage and even man-made structuring.

## 1. Introduction

Many naturally occurring surfaces have functional efficiencies equal to or, in some cases superior to, man-made technologies [1–4]. Some naturally occurring nano-structures (of both plant and animal origin) demonstrate self-cleaning hydrophobic/superhydrophobic 'technologies' that have been finely tuned to aid in species survival [5,6]. Of particular interest is the structuring of the lotus leaf which easily sheds water (from rain and fog) from the leaves which can carry away contaminants from the surface [6,7]. Other examples include the cuticle (or cuticular products) of a range of insects (e.g. cicada, lacewings, dragonflies and planthopper) where the wings have specific and unique structuring that allows them to shed contaminants and water very easily [5,8–11].

A number of other living organisms demonstrate unique abilities to keep their surfaces clean of dirt and other contaminants. For example, geckos (small lizards), some of which have small stalk-like projections (spatula) on their feet which allow them to stick to natural and artificial surfaces (e.g. rocks, foliage, walls and ceilings) also demonstrate self-cleaning properties [12]. Contact mechanical models of the gecko feet structuring have suggested that the self-cleaning occurs by an energetic disequilibrium between the adhesive forces attracting a dirt particle to the substrate

and those attracting the same particle to the spatula [12]. As well, the predicted cleaning force on contaminant particles may be significantly increased via digital hyperextension [13]. These micro-/nano-structures of the gecko foot have been extensively studied by numerous researchers (predominantly from the species *Gekko gecko*) [14–19] and even a product based on their structuring has been developed (Gecko adhesive).

While the feet of some geckos have attracted significant interest, the remaining regions of the lizard body have received little attention in relation to adhesive properties, especially those related to solid contacts, which adds to the impetus for investigations of such topographies and associated functioning. Interestingly, the outer layer of lizard skins has been shown or speculated to, exhibit a range of functions including ecdysis, coping with varying temperatures, pheromone capture, retention and dispersal, tribological functions such as reduction of friction and wear protection, and also reflection of radiation (e.g. [20]).

Self-cleaning of natural structures can take place by a variety of mechanisms including active removal by organism appendages and also environmental factors such as the action of water (e.g. rain) or wind. It has also been suggested that self-cleaning plays an important role in the defence against pathogens, such as spores, bacteria and fungi and conidia of pathogenic microorganisms. Indeed, many studies have shown that numerous lizards are susceptible to various external contaminants which can cause serious skin problems/diseases [21]. Maintaining the surface properties of the gecko skin free from contamination may be potentially beneficial for a number of reasons. Contamination remaining on the surface may act as a nucleation point for further solid contamination (e.g. bacteria and fungi). It may also change the wetting properties of the skin allowing water to remain on the surface for longer periods. As the growth of many microorganisms is provided by permanent or temporary water availability, proliferation may result from wetting property changes.

The atmospheric and terrestrial environment surrounding geckos contains a multitude of inorganic, organic, biological and anthropogenic particulate matter which can potentially contaminate the outer lizard skin; for example, dust and plant material. Pollen grains are generally the most abundant component among the floating particles in the air (aeroplankton) surrounding most terrestrial organisms including human beings [22]. Other potential airborne and terrestrial contaminants can originate from soils. Naturally occurring silicate particles composed principally of silicon dioxide ($SiO_2$) such as quartz can make up as much as 90–95% of the sand and silt fraction of soil [23]. Both pollen and silica have a range of associated health aspects for humans (e.g. trigger symptoms of allergic respiratory diseases such as asthma and hay fever, lung cancer, lung disease, silicosis, pulmonary tuberculosis, emphysema and immunologic reaction (e.g. [24–27]). Thus, enhanced mechanisms for shedding contaminants such as pollen and silica particles are of great interest. As well, interaction of these particles with various surfaces is of significance in terms of distribution, transport and capture of these contaminants.

As well as the health concerns associated with silica and pollen, these bodies also represent a ubiquitous source of hydrophobic and hydrophilic particles which come into contact with the gecko. The need for geckos to maintain functionality of the outer skin upon exposure to such contaminants suggests that there may be some structural components which facilitate mechanisms to aid in particle removal. The gecko skin is shed periodically (up to time periods of several months) and thus it is necessary to maintain its integrity and functionality for considerable time periods.

In this study, we have measured micro-/nano-adhesion of a range of potential airborne and ground contaminating particles on the outer skin of the gecko *Lucasium steindachneri*. This includes both natural (pollen grains) and anthropogenic model particles (silica, and $C_{18}$ particles). This particular gecko is generally ground dwelling and inhabits semi-arid regions, which suggests that removal of contamination may not always be possible via a water removal mechanism. As well, unlike the gecko foot where the frequency of contact with the substrate is high and is sufficient to remove particles, the gecko skin (especially dorsal regions) will not come into contact with foreign substrates to the same extent thus environmental mechanisms (e.g. wind, rain and fog) may be primarily responsible and/or required for self-cleaning.

## 2. Experimental procedure

### 2.1. Gecko capture and preparation

Box-patterned geckos (*L. steindachneri*) were captured at night by hand, from the Mingela Ranges (20°08′06″ S, 146°52′32″ E), Queensland. Only healthy, adult lizards were returned to the laboratory, held in plastic containers with a heat source for thermoregulation, paper towel as substrate (changed weekly), a small tree branch and water ad libitum. They were fed domestic European crickets (*Acheta domestica*) three times a week. Geckos were allowed to shed twice before experiments were conducted. Lizards were euthanized to ensure the skin's surface was intact and undamaged. Lizard skins were surgically separated by scalpel, cut into smaller sections ($1–5 \times 1–5$ mm$^2$) and attached to glass slides for adhesion experiments.

### 2.2. Adhesion experiments with contaminants

The adhesion measurements were carried out with an atomic force microscope (AFM); ThermoMicroscope TMX-2000 Explorer. The instrument is based on detection of tip-to-surface forces through the monitoring of the optical deflection of a laser beam incident on a force-sensing/imposing lever. The analyses were carried out under air-ambient conditions (temperature of 24–26°C and 70–75% relative humidity).

Tipless beam-shaped levers (diving board in shape—NT-MDT Ultrasharp) were used throughout the work. The attachment procedure of the silica, $C_{18}$ and pollen particles to the lever has been described in the literature [8]. The pollen grains and silica particles were characterized by optical microscopy and scanning electron microscopy (SEM). Only pollen grains with no observable damage upon fixing to a lever were used for adhesion measurements. Force versus distance ($f$–$d$) analysis was used to obtain adhesion data. The probe is held stationary at an $x$–$y$ (sample plane) location and is ramped along the $z$-axis, first in the direction of approach and contact with the surface, and then in the reverse direction. $F$–$d$ curves were acquired at rates of translation in the $z$-direction in the range 5–10 μm s$^{-1}$. Each $f$–$d$ curve consisted of 600 data points.

Forty measurements per particle were acquired for each location. A total of four particles were attached to cantilevers for each particle type (i.e. four silica (Bang Laboratories), $C_{18}$ beads (Nova-Pak® $C_{18}$) and specific pollens (*Tridax procumbens*

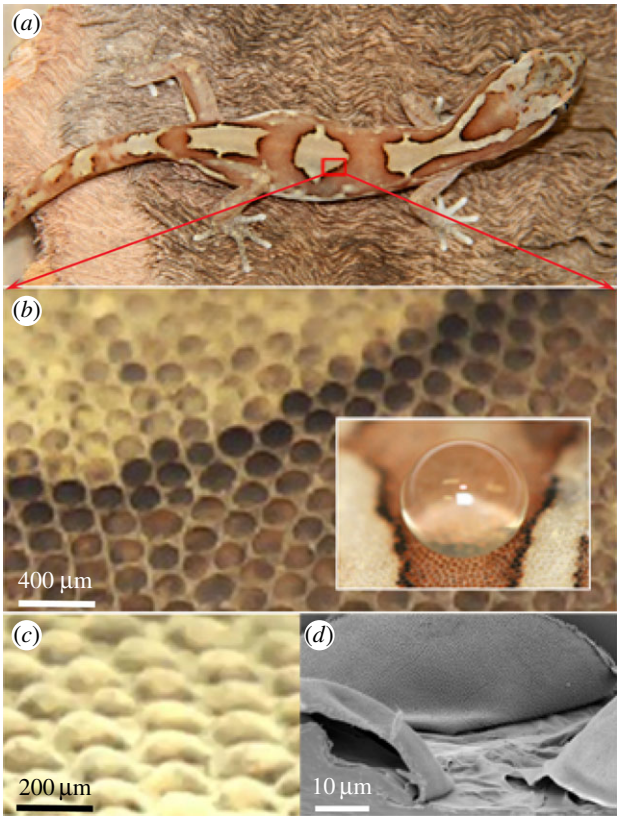


**Figure 1.** (*a*) Photo of the gecko *L. steindachneri* (box-patterned gecko). (*b*) Optical image showing the micro-structuring of the outer skin on the dorsal region of the gecko. These regions primarily consisted of dome-shaped scales in a relatively close-packed hexagonal patterning (inset: a water droplet demonstrating a superhydrophobic interaction). (*c*) Optical image of the dorsal back region showing the scales projecting above the surface. (*d*) Topographical SEM image of the epidermal dome regions (scales) on the dorsal area of the lizard. (Online version in colour.)

(daisy), *Euphorbia leucocephala* (Snowflake), *Grevillea longistyla* × *Grevillea venusta* (Firesprite), *Hibiscus rosa-sinensis* (Hibiscus), *Acacia aneura* (Wattle), equalling a total of 160 measurements per particle type) were used for adhesion measurements, each yielding 40 measurements for each sample. In addition, two silica 30 µm diameter beads (Microspheres–Nanospheres) were used for adhesion measurements on the gecko dorsal region. The normal force constant of the probe was determined by using resonance methods and the scanners were calibrated using atomically flat surfaces [28]. The raw adhesion values were then entered into SigmaPlot v. 10.0, whereby standard error values were obtained and presented as error bars.

Adhesion was measured under the conditions of the two surfaces coming into contact with no applied loading force (i.e. adhesion represented the force of attraction that the particle surface would experience where deformation of structures is minimized and where the main contributing force involved is simply that of the adhesion of the particle to the surface). Adhesion was also measured for some samples with a controlled maximum applied force loading to investigate adhesional changes under such conditions. The preparation procedures of insect samples for adhesion experiments were the same as used in the literature [8].

### 2.3. Scanning electron microscopy

In the case of SEM imaging (figures 1 and 2), a small section of lizard skin (approx. 3 × 5 $mm^2$) was excised and mounted on an aluminium pin-type stub with carbon-impregnated double-sided adhesive, then sputter coated with 7–10 nm of platinum, before being imaged using a JEOL 6460 or 7001 SEM at 8 kV. The same conditions were used for insect cuticle examination.

## 3. Results and discussion

### 3.1. Skin characterization of the gecko

The gecko examined in this study (box-patterned gecko—*L. steindachneri*) is shown in figure 1*a*. Adult specimens are generally 50–60 mm in length with a small mass of approximately 2.5 g [29].

Previous studies have investigated the oberhautchen (outer thin layer) of numerous lizard skins including some geckos and determined the presence primarily of β-keratin [30,31]. X-ray photon electron spectroscopy (XPS) data of the gecko skin used in this study also suggest that keratin is a component of the dorsal and abdominal regions (see electronic supplementary material for XPS information and figure S1 for further details).

The micro-structuring of the outer skin was examined on the dorsal back and abdominal regions with optical and SEM. These areas primarily consisted of ordered dome-shaped scales with varying pigmentation (figure 1*a–c*). For example, on the lizard dorsal regions, the scales were typically 100–190 µm in diameter with a similar centre-to-centre spacing and height in excess of 50 µm. Figure 1*d* shows a topographical SEM image of the microstructure showing scales from the dorsal region. The abdominal (ventral) regions exhibited a similar micro-structuring. The inset shown in figure 1*b* demonstrates that the topography facilitates a superhydrophobic interaction with water. Static water contact angles confirm this and are typically between 151 and 155° on both the dorsal and ventral regions of the gecko.

Higher resolution SEM images of the gecko surface for the dorsal (back and head) and ventral (abdominal) regions are shown in figures 2 and 3. The gecko skin consists of micro-structuring featuring spinules (small hairs) with lengths up to 4 µm. These spinules are present on the scale area as well as regions between the scales (troughs). The termination of the spinules can be described as spherically capped with over 98% having a small radius of curvature (less than 30 nm) typically in the range of 10–20 nm. The density of spinules is very high; up to 500 per 10 × 10 $\mu m^2$ area resulting in a sub-micrometre spacing of these hairs (figures 2 and 3). Spinules have been reported on some gecko species ranging from 0.2 to 0.7 µm in spacing and varying heights [32–36]. Interestingly, the higher resolution SEM images of scale and trough regions (from the head, dorsal and ventral regions—figure 2) show a clear distinction. The regions marked ii, iv and vi show images of the trough regions (between scales). These regions exhibit spinules with a consistent height and spacing. By contrast, the scale regions marked i, iii and v show an array of spinules of varying heights consisting of two distinct lengths comprising short and longer spinules with a similar spacing.

Figure 3 also highlights the topographical differences between the scale and trough regions on the gecko. It is apparent that the trough regions (figure 3*a–c*) consist of areas which exhibit significant folding of the skin. By contrast, the scale regions (figure 3*e–g*) show very little evidence of folding. As well, the scale regions typically demonstrated a more

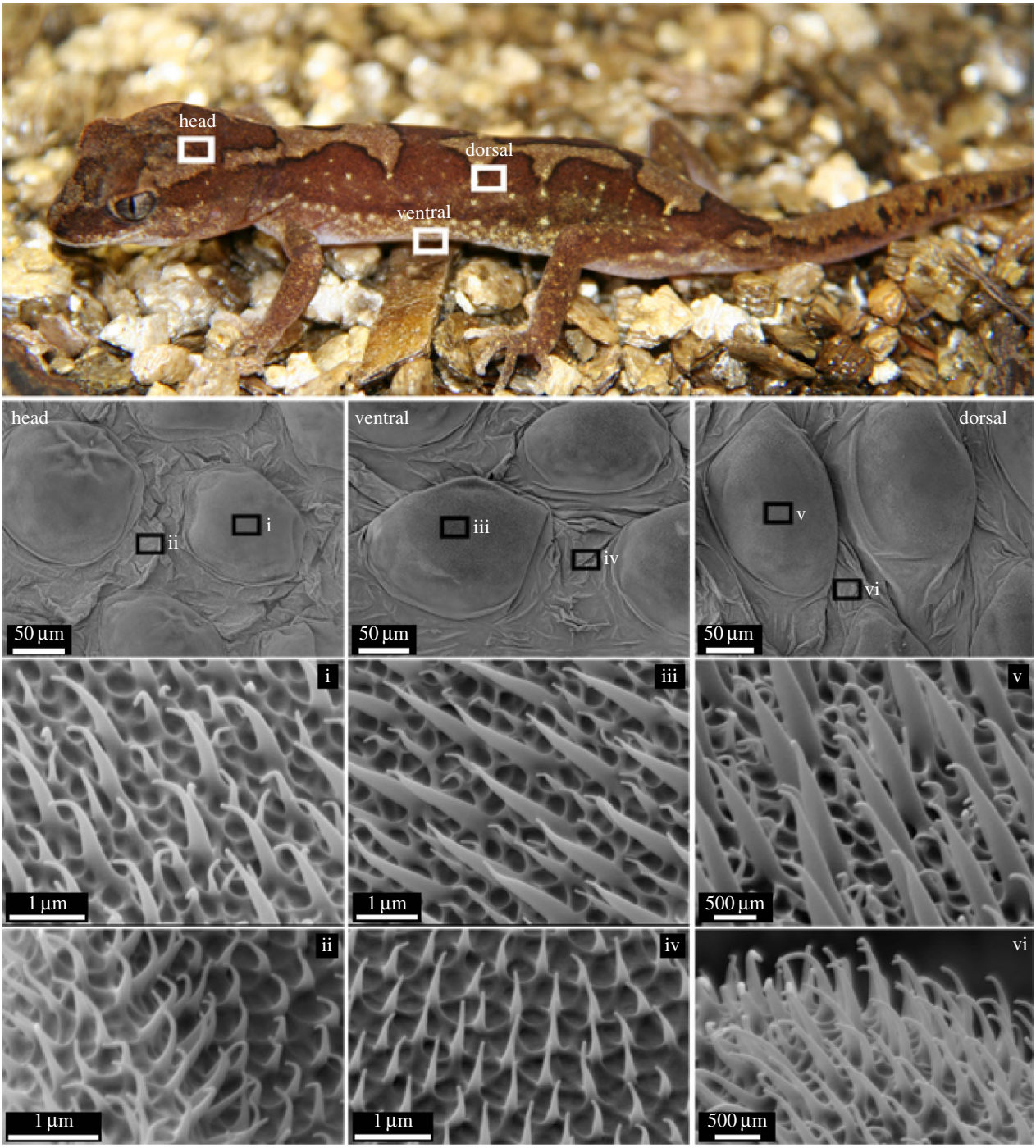


**Figure 2.** SEM images of the microstructure on the dorsal, head and ventral regions of the gecko. The regions marked i, iii and v show images of the scale regions at various magnifications. The regions marked ii, iv and vi show images of the trough regions (between scales). The scale regions show an array of spinules of varying heights (two distinct size ranges) while the trough regions exhibited spinules of a consistent height. (Online version in colour.)

defined base structuring which consisted of many small interconnecting raised structures (typically circular and at times near hexagonal in shape forming micro-sized rib structuring (figure 3*g*)). One may speculate on the differences in general architecture of the scale and trough regions on the gecko. The heavily folded trough regions may stretch and fold to accommodate movement of the lizard which can adopt significant body conformations (see electronic supplementary material, figure S2). The folding may also potentially accommodate for growth between skin shreds. The absence of folding on the scales suggests that these areas may be more structurally rigid. The more pronounced underlying rib-like (honeycomb in appearance) structuring at the base of the scales below the spinules may also aid in structural rigidity with minimal cost in terms of material formation. As the scales are more likely to come into contact with environmental structures, a more rigid and higher tiered structuring (three layers/tiers of structuring) may present a more durable architecture to maintain integrity and levels of wear resistance.

A schematic illustration of the two-tier trough regions (folding of skin and consistent spinule height) and the three-tier scale regions (rib structuring and two distinct heights of spinule arrays) is shown in figure 4. Based on this structuring, one would predict that one of the functions of the architecture could be related to reducing adhesional contact with contaminating bodies. With this in mind, we have measured the adhesion of a range of contaminants which could potentially interact with the skin surface.

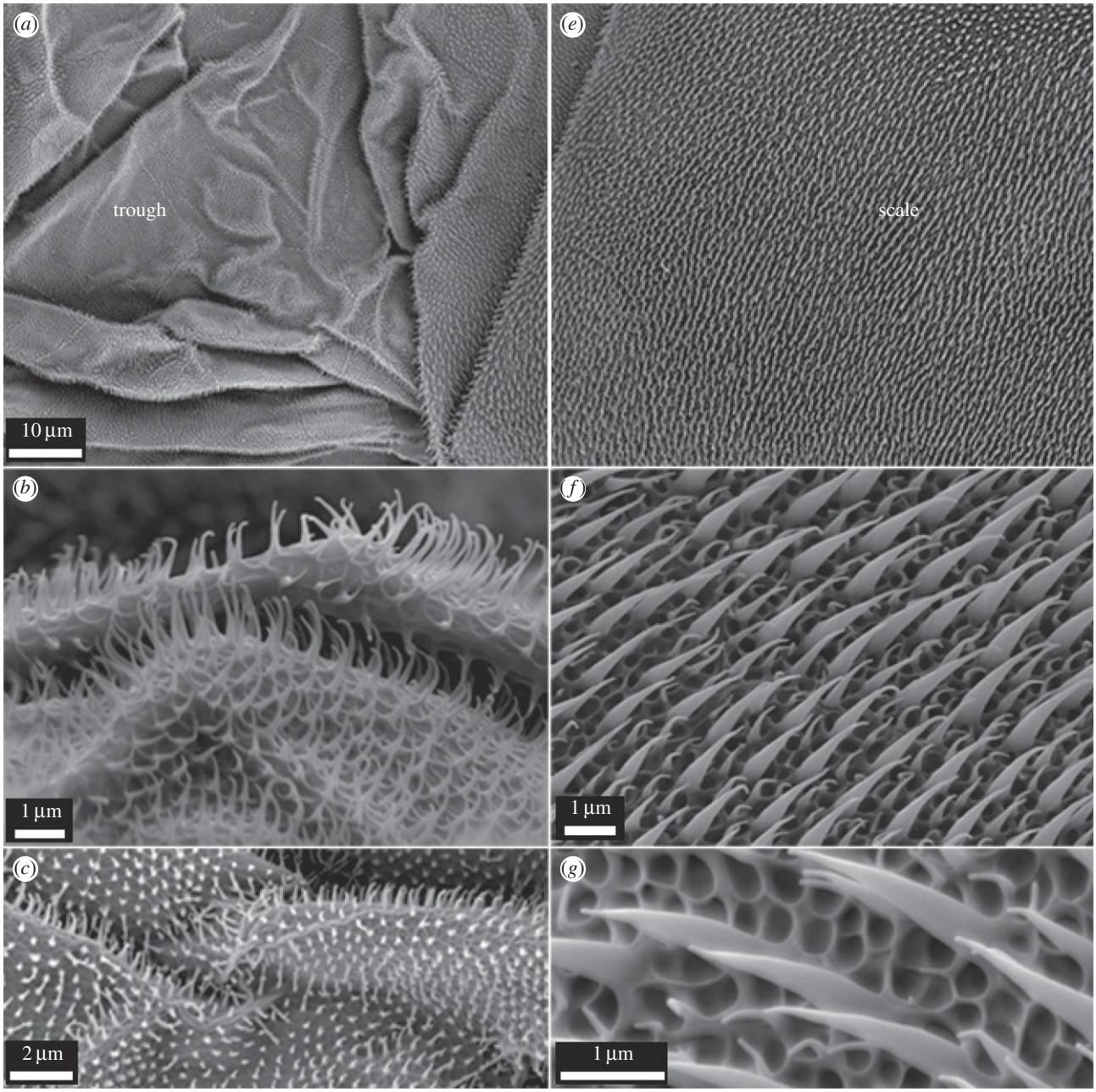


**Figure 3.** SEM images of the scale and trough regions on the gecko. The trough regions (*a–c*) show heavily folded areas with a two-tier structuring (folded areas and spinules). The scale regions (*e–g*) demonstrate a three-tier hierarchical topography consisting of an array of spinules of two heights and an underlying honeycomb (rib-type structuring).

## 3.2 Adhesion of contaminant particles on the gecko skin

Seven different particle types (contaminants) have been used to measure adhesion on the gecko skin. Two of these comprised silica and $C_{18}$ particles representing contaminants of hydrophilic and hydrophobic origin. These particles were roughly spherical having a similar radius of curvature. Five other particles (whole pollens) were chosen to mimic contact conditions of natural particles which could potentially contaminate the structured gecko surfaces. The pollens were chosen based on their size differences, distinct topographies, levels of roughness and locational distribution. The outer layer of pollen grains have been shown to comprise carboxylic acids cross-linked with saturated and unsaturated aliphatic chains with varying amounts of aromatics resulting in a hydrophobic surface (e.g. [37]).

Figure 5 shows SEM images of the pollen and particles (coloured to enhance features) and their finer surface topographies used for adhesion measurements. The silica particle (*f*) has a nano-roughness below 10 nm RMS while the $C_{18}$ spheres (*g*) have a higher roughness with asperities typically around 100–200 nm in lateral and height dimensions. As shown in figure 4, two pollens (*a* and *e*) have a spherical shape with a number of spikes protruding from the surface. The *T. procumbens* daisy (*e*) has spikes (more than 100) with diameters of approximately 500 nm and heights in excess of 3 µm. The other spherical pollen (*a*—*H. rosa-sinensis*) has spikes (approx. 50–60) with a diameter an order of magnitude larger in size (approx. 5 µm in diameter and 20 µm in height). The *A. aneura* (wattle) pollen (*c*) demonstrated a patterned surface with furrows and a relatively flat topography at the micrometre scale. The snowflake pollen, *E. leucocephala* (*d*) demonstrated a

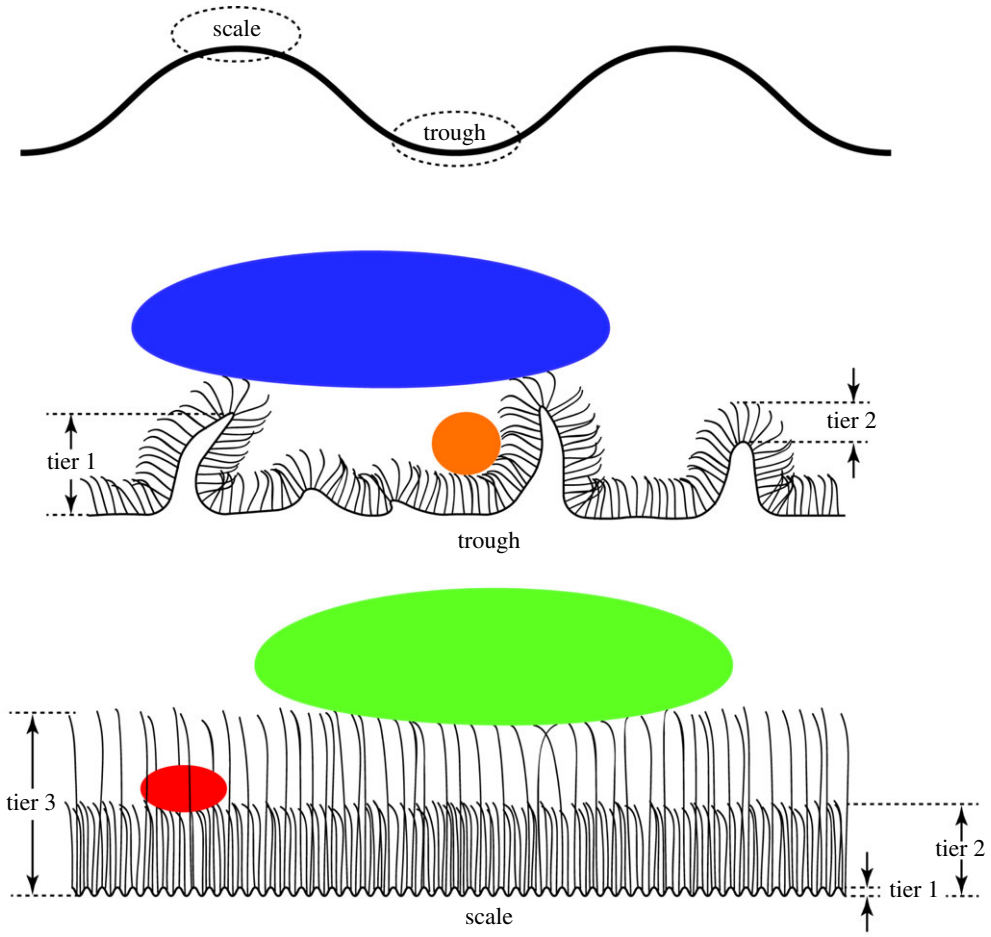


**Figure 4.** Diagrammatic representation of the scale and trough regions on the gecko body showing the two-tier structuring on trough regions and three-tier structuring on the scale regions (not to scale). The predicted influence on contact area of contaminating particles of different length scales is also shown. (Online version in colour.)

homogeneous surface topography/roughness on all sides comprising a netting structure with small holes.

The adhesion of contaminants (pollen grains, spherical silica and $C_{18}$ particles) on the dorsal, head and ventral regions of the gecko was measured using AFM. The AFM is ideally suited for particle adhesion measurements in air or aqueous environments [8,38,39] and on the cuticle/skin of organisms [8,39]. The processed data are shown in figure 6. In order to place the value of the various particle adhesions into context, the contaminants were also interacted with a range of other surfaces including a near atomically flat silica surface and insect cuticles. These surfaces have distinct topographical characteristics and wetting properties (see also electronic supplementary material, figure S3). The insect wing cuticles were selected for comparison as they represent surfaces which have been previously studied and found to exhibit (depending on the species) extremely low adhesion with contaminants or alternatively higher adhesion [8,39]. Generally, insect wings demonstrate very low adhesion as contaminates can potentially interfere with functional efficiency (for example flight efficiency and changes in reflective properties of membrane) [8].

The adhesion between the silica particle and the gecko skin represents a high surface energy contaminant particle coming into contact with the low energy spinule arrayed surface. There was a significant difference in adhesion of the silica particle with the gecko skin compared with the flat silicon surface (silicon wafer with an oxide layer). Adhesion of such particles was over 20 times greater than on the lizard surface (less than 30 nN on the gecko and almost 700 nN on the flat silicon). If we model the terminal end of the spinule surface as a spherical section, the interaction energy between a spherical particle and a spinule end [40] is given by the following equation:

$$W_{(D)} = \frac{-A}{6D}\frac{R_s R_p}{(R_s + R_p)}, \tag{3.1}$$

where $A$ is the Hamaker constant (typically $10^{-19}$ for van der Waals interactions in air), $R_s$ is spinule radius, $R_p$ is the particle radius and $D$ is the separation distance.

The adhesional (pull-off force) $F_{sp}$ of the spinule terminus from the particle can be approximated using a minor variation of the Johnson–Kendall–Roberts model [41].

$$N_{sp}F_{sp} = N_{sp}\frac{3}{2}\pi R_e W_{sp}, \tag{3.2}$$

where $N_{sp}$ is the number of spinules in contact with the particle, $W_{sp}$ is the work of adhesion between the two surfaces and $R_e$ is the reduced radius

$$R_e = \left[\left(\frac{1}{R_s}\right) + \left(\frac{1}{R_p}\right)\right]^{-1}.$$

As the particle radius is over two orders of magnitude larger than the spinule radius, the reduced radius approximates to the spinule radius. By using a value of $W_{sp}$ of 20 mJ m$^{-2}$ [42], the pull-off force for one spinule with the silica particle will be approximately 1 nN. The adhesion range measured on the gecko of 10–30 nN suggests that the particle makes contact

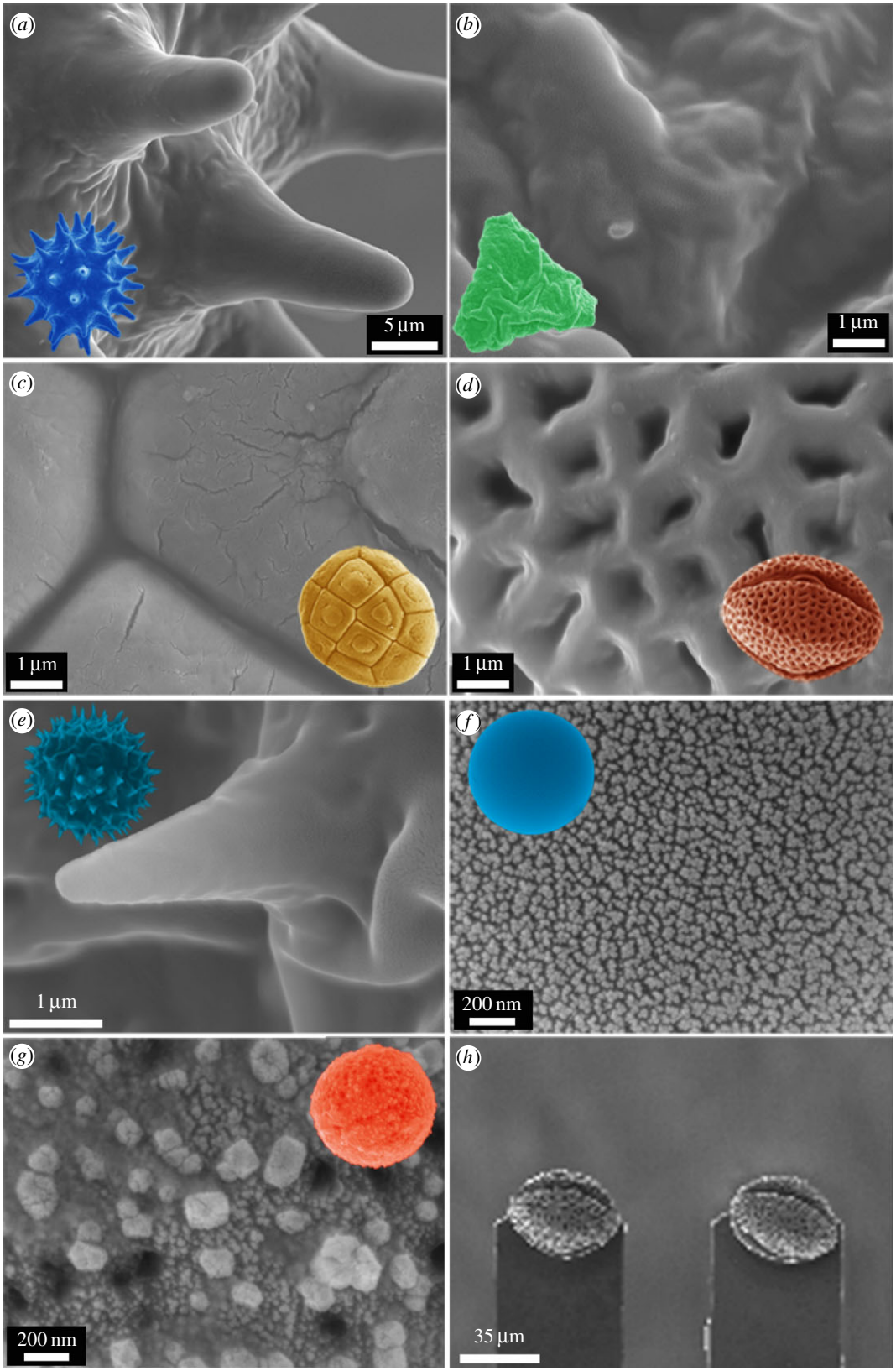


**Figure 5.** SEM images of the particles used for adhesion measurements and their finer surface features used in the study (*a*–*g*). The insets provide a visual reference of particle type (refer to part (*a*)). (*h*) An example of the typical resulting orientation of pollens (pollen (*d*)—snowflake (*E. leucocephala*) in this case) on AFM cantilevers. Only pollens exhibiting similar orientations were used for adhesional measurements. (Online version in colour.)

with numerous spinules. However from figures 2 and 3, it is clear that the particles may also make contact with regions of the spinules (due to the orientation of the spinule near the tip) other than the apex. This may result in an increased contact area and adhesional contact in comparison with a model spherical spinule—particle interaction. Adhesion measured on the gecko skin with a 30 µm diameter silica particle on the dorsal region of the gecko yielded an adhesion of approximately 150–200 nN. This reflects the increase in contact area of the particle interacting with significantly more spinules on the skin surface.

Adhesion of the $C_{18}$ particles with the gecko skin was less than with the comparably sized silica particles (compare data for 5 µm particles; figure 5). The interaction force of the $C_{18}$ particle is one order of magnitude less than the equivalently

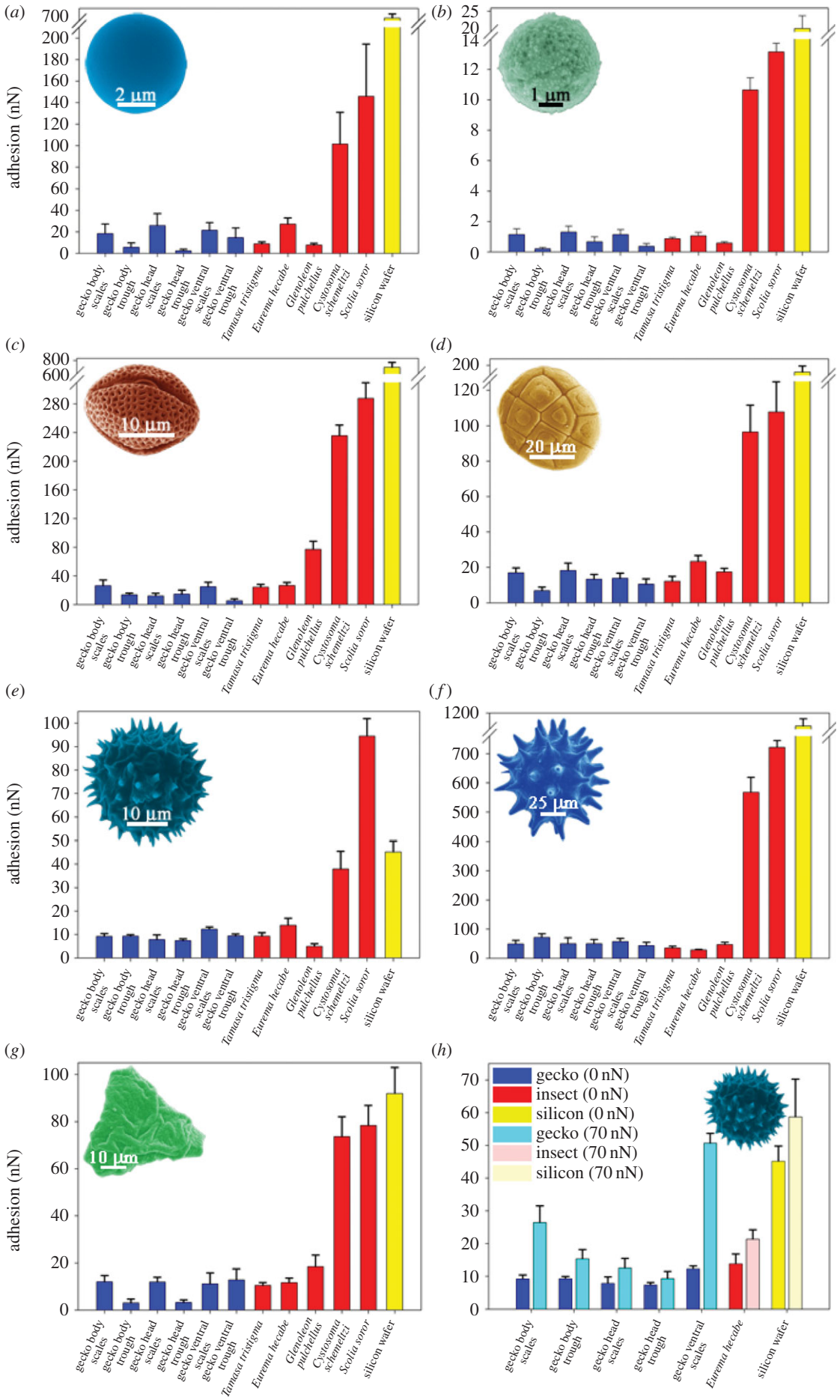


**Figure 6.** (*Caption Opposite.*)

**Figure 6.** (*Opposite.*) Adhesion measurement values (in nN), using AFM probes of various pollen and spheres, interacting with the gecko dorsal (body), head and ventral skin regions at locations on the scales and areas between the scales (troughs). For comparison, other surfaces are also illustrated including insect wing membranes which have previously demonstrated ultra-low adhesion and high adhesion. The topography and measured static contact angles for the insect surfaces are shown in electronic supplementary material, figure S3. (*a*) Interactions of silica particles, (*b*) $C_{18}$ partciles, (*c*) *E. leucocephala* Snowflake bush, (*d*) *A. aneura* wattle, (*e*) *T. procumbens* daisy, (*f*) *H. rosa-sinensis*, (*g*) *Grevillea longistyla* × *G. venusta* grevillea Firesprite cultivar; (*h*) the comparative adhesion at two distinct force loadings of *T. procumbens* on the gecko and other surfaces. Note that (*a–d*,*f*) contain axis breaks as a result of the very high adhesional values between the particle/pollen and Silicon wafer. Error bars—standard error values. (Online version in colour.)

sized silica particle. This represents the difference in adhesion of a relatively rough hydrophobic and smooth hydrophilic particle coming into contact with the skin.

The pollen grains used showed a higher adhesion on all surfaces in comparison with the $C_{18}$ particles; however, the values are comparable with the silica particle. This reflects the much larger size of the pollens. For example, a single asperity on the *H. rosa-sinensis* pollen is of a similar size in diameter (approx. 5 µm) to the silica particles. The pollen grains can also make multiple contacts with the lizard skin via a number of the outer projections. Generally, the rougher morphology and more hydrophobic nature of the long chain polymers that composes the pollen sporopollenin (outer layer) yield a low adhesion. The spherical shaped pollen profiles with small asperities, *A. aneura* wattle, exhibited the lowest adhesion. By contrast, the largest pollen, *H. rosa-sinensis*, will interact with less asperities however the contacting area will be higher due to the significantly larger dimensions of the pollen spikes.

The adhesional responses of particles with the various surfaces were also measured at an applied loading force as opposed to the situation where the two surfaces just make contact (approx. zero applied force). Adhesional increases can potentially take place by increasing the contact area of asperities with spinules and/or the number of asperity spinule contacts. As the loading force is increased, both of these factors are likely to increase. Figure 6*h* shows the effect of increasing the loading force of the particle–spinule contact with an applied force of 70 nN with the *T. procumbens* daisy pollen. This applied force can increase the adhesional force on the gecko skin by over twice the value measured at zero force loading (figure 6*h*). As the adhesional force also increased when the pollen underwent an additional loading force on an infinitely hard surface (silicon wafer) some component of the increased adhesional force shown in figure 6*h* may be a result of deformation of the pollen particle asperities.

The particle adhesion on the gecko is in the same range as measured on the superhydrophobic insect cuticle membranes (figure 6). For example, adhesion values are of the same order as the superhydrophobic cicada wing cuticle which has demonstrated one of the lowest adhesion measurements of a natural surface [8,39]. All of the hydrophilic insect wings demonstrated a higher adhesion than the gecko skin for all particles. The highest adhesion between hydrophilic insect membranes and a pollen (*H. rosa-sinensis*) was over 500 nN.

From figures 2 and 3, and highlighted in figure 4, the scale and trough regions on the gecko have different hierarchical topographies (distinct three-tier on the scale and two-tier on the troughs). Based on this contrasting topography, we measured adhesion specifically on these areas (figure 6). The adhesive force on the scales and the troughs showed a distinct contrast for most of the particles. Adhesional forces, for example, of the silica particles (figure 6*a*) on the scales were significantly higher than that on the troughs of all other areas (body, head and ventral regions). This trend was also evident on the carbon particle (figure 6*b*) and all pollens, except for the two pollens which comprised asperities. From figures 2 and 3, it is apparent that the topography of the troughs is significantly rougher than the scale domes, consisting of the folding of the skin. Thus, the contact area of particles is reduced in the troughs as a consequence of minimizing the number of individual contacts with the spinules with a corresponding reduction in adhesion (figures 4, 6 and 7). The two pollens with asperities *H. rosa-sinensis* (figure 4*b*) and particularly the *T. procumbens* daisy (figure 4*f*) have the required topography (spikey projections) to access regions on both scale and trough topographies. Thus, one may expect less of a difference between the two regions which is observed in the measurements. As well, the larger pollen (*H. rosa-sinensis*) is of comparable dimensions to the spacing between scales (figure 7). Consequently, trough adhesion measurements may also have contributions from interactions with the scale sides as well as trough regions as is illustrated in figure 7).

Several studies have investigated the adhesional forces of varying contact area (the use of probes of varying radii of curvature) with hierarchical natural and fabricated surfaces. Although many do not state a loading force for their contact conditions, they do however all demonstrate the varying degree of contact area dependence on adhesion. Natural plant surfaces, such as the Lotus leaf (*Nelumbo nucifera*), *Colocasia esculenta*, Nasturtium (*Tropaeolum majus*) and Ryegrass (*Leymus arenarius*), all demonstrate a two-tiered hierarchical micro-/nano-structuring with adhesion values ranging between 70 and 330 nN interacting Si, and borosilicate spheres (with various chemical coatings) of 15 µm radii of curvature (e.g. [43,44]). One paper [43] quotes an applied force loading of 50 nN, measuring an adhesive force of *ca* 330 nN.

Adhesion measurements have been carried out on a number of fabricated micro- and nano-structures. Some of these fabricated surfaces have demonstrated low adhesion values between particles with varying radii of curvatures (from 20 nm up to 30 µm) with values as low as approximately 15 nN [45–47]. In addition to the particle adhesions described above in our study, we also measured adhesion at a 50 nN applied force on the gecko skin using a silica bead of 5 µm in diameter with an adhesion less than 5 nN (lowest value recorded on gecko trough regions) and 50 nN (highest recorded value on scales) with an average value of approximately 28 nN on the gecko skin. Burton & Bhushan [47] measured adhesion on a PMMA nanopillar surface with a slightly larger spacing and tip apex diameter to the gecko spinules (approx. 500 nm spacing and 100 nm diameter near the apex on the PMMA) and measured an adhesion force of approximately 120 and approximately 175 nN for a 7.6 µm and 30 µm diameter silica sphere, respectively. However equivalent nanopillars comprising hydrophobic coated PMMA pillars (e.g. perfluorodecyltriethoxysilane (PFDTES)) showed comparable adhesion values (approx. 35–50 nN for the PFDTES, 7.6 and 30 µm coated spheres) to our study on gecko spinules.

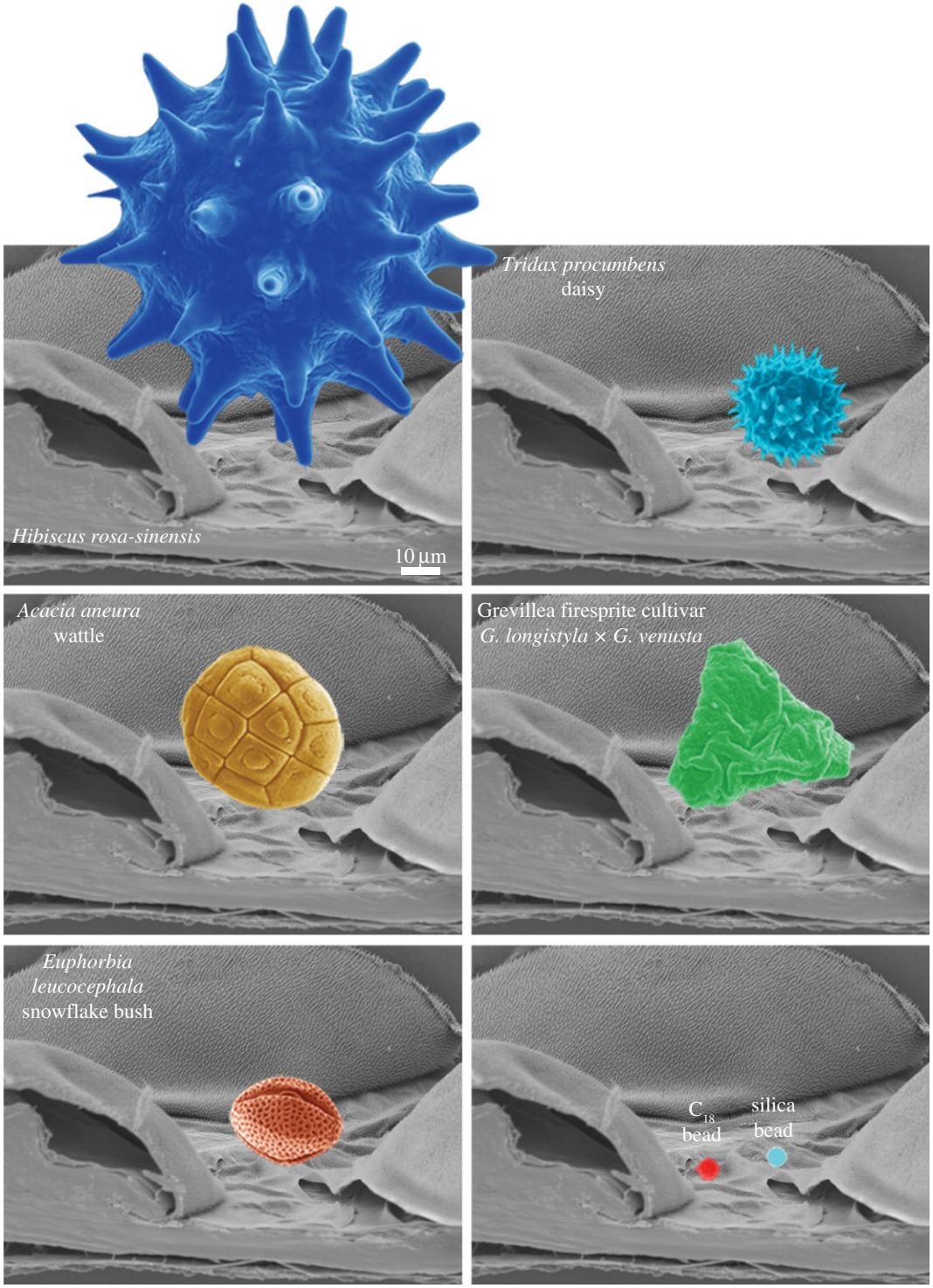


**Figure 7.** Images showing the relative sizes of the particles with the gecko scale and trough regions. The figure also reflects the potential areas of contact between the various pollen and beads with the underlying gecko skin (contact with the wrinkly trough and scale dome regions). (Online version in colour.)

The adhesion responses (by viewing the AFM force–distance curves) on different surfaces can be used to interpret a variety of surface properties and structure (e.g. [48]). Analysis of the fine structure of the force–distance curves for various particles showed a variety of interactions (figure 8). Typically when the particles interacted with a flat surface such as the silicon wafer, they were characterized by a single release point from the surface (see the three curves at the top of figure 8). When the particles interacted with the gecko spinule surface, however, multiple releases from the surface were often observed as highlighted by the dashed square boxes denoting this feature in figure 8. Thus, the particle may remain adhered to a spinule and/or spinules after it has been released from other spinules on the skin. The smallest release points observed for particles were below 1 nN. For the silica bead interacting with the spinules, the lowest values were in the range of 1–3 nN, which is of the same order as predicted in equation (3.2) for such interactions.

Another interesting feature seen in figure 8 is the change in gradients of the force–distance extension/retraction region of the curves on the gecko as highlighted by dashed circular areas. The reduced gradients may indicate a variety of interactions. For example, it may imply that the spinule orientation has changed during the retraction event (for instance, the

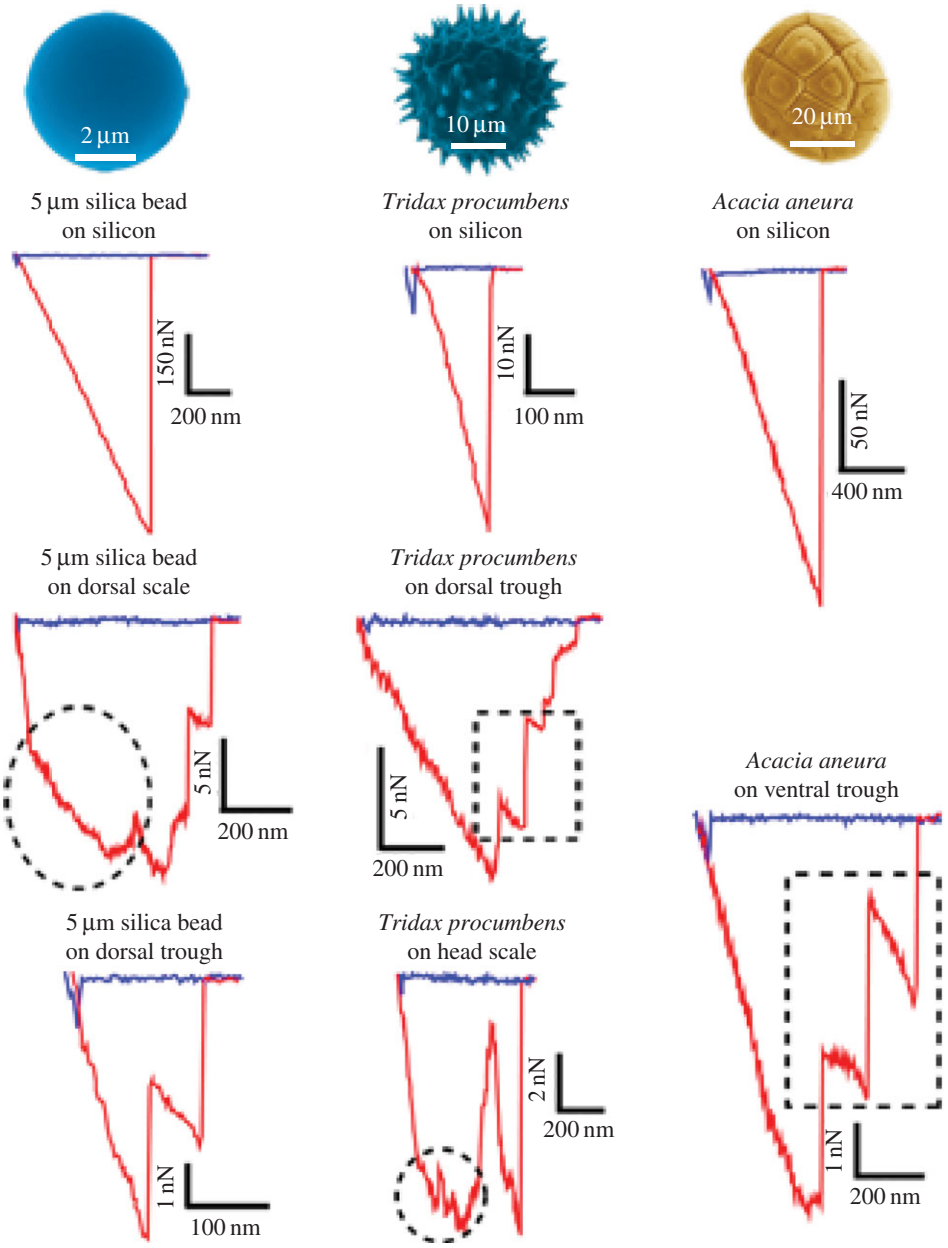


**Figure 8.** Examples of force versus distance curves demonstrating fine structure of the adhesional contacts. The approach part of the cycle is shown in blue (with some distinct snap-on features where the surfaces make contact), while the retract part is shown in red. The retraction shows a number of features such as possible multiple releases from the surface (e.g. dashed square boxes) and the change in gradients of the force–distance extension/retraction region of the curves (e.g. circular dashed sections). The reduced gradients may indicate a variety of interactions as discussed in §3.2. (Online version in colour.)

spinule or spinules is/are pulled into a more vertical position from an initially inclined orientation). Another possibility is the particle sliding along the spinule/s during the retraction process. Future studies involving the mechanical properties of the particles (especially pollens) and the spinules may shed further light on the variety and nature of such fine structure observed in such interactions.

## 3.3 Adhesional considerations of the spinules for interaction with environmental substrate surfaces

While the adhesion of individual spinules with contaminating particles is very low, contact situations with other much larger solid bodies which the gecko can potentially interact with is also of interest. In such cases, contributions of many thousands of individual spinules (especially on the abdominal surface and if deformation occurs) may need to be considered. While the adhesion of an individual spinule from our study is an order of magnitude less than that reported for an individual gecko foot spatula (approx. 1 nN compared with 10 nN; e.g. [42]) the potential contact area of scales (and thus number of spinules) may make this adhesional force contribution significant. As the spinule dimensional parameters on many species of gecko are similar [32–36] to those in our study, a comparable adhesion with surfaces is likely in many cases.

Of note is the potential for this contribution to provide additional adhesional capabilities (sticking ability) for some gecko species when interacting with environmental substrates such as rocks, foliage and even man-made structuring. We have observed, on a numerous occasions that some gecko species (e.g. *Hemidactylus frenatus*, the Asian house gecko), while resting on inclined surfaces, e.g. walls, tend to keep their bodies and tails flat against that surface (see electronic supplementary material, figure S4). This behaviour may aid in increasing the stability of the lizard by increasing the

number, locations and distribution of adhesional focal points. Thus, the adhesion provided by the foot structuring may be augmented by spinule contacts. As such, this action may aid in the gecko increasing its already firm grip reducing the chances of falling and potential injury or attack from predators in the process. We have previously looked at the interaction of water droplets with the gecko skin and suggested that around 100 000 spinules may be in contact with a small water droplet of a few millimetre in diameter [49]. Thus, it is not unreasonable to envisage more than $10^6$ spinules contacting a substrate from the ventral region of the gecko body. A resulting adhesion of 1 mN is not negligible for a gecko of only several grams in mass where a gravitational force of approximately 20 mN acts upon the body. Minor deformation of spinules may increase this adhesional force contribution.

## 4. Conclusion

The gecko is one of the smallest of all lizards and thus the epidermal surface area is also small; however, the skin surface area to body mass/volume ratio compared with larger lizards is high. This may indicate (based purely on dimensional considerations) that the gecko is potentially more susceptible to the effects of contamination and infection and/or disease.

The hierarchical and open-framed intricate architecture of the gecko (with its distinct two- and three-tier topographies) suggests that the surface structuring of the gecko may facilitate minimal adhesion with particles of various length scales by minimizing the number of contact points and contact area. We have evaluated the contact forces of various contaminating bodies by measuring the strength of interaction between particles with the gecko micro-/nano-structuring. Low adhesional forces were measured for all particle sizes and chemistry on the scales and trough regions. However, higher adhesion was measured on the scale areas for most particle types. The slight increase in adhesion of the scale regions and observation of some gecko species contacting substrates with their abdominal regions may suggest that additional adhesion is provided to augment foot gripping in some circumstances. Further adhesion experiments on geckos where adhesional grip is important (e.g. arboreal species) should elucidate this contribution. The trough locations where folding of the skin occurs, presents a limited contact domain for interacting particles by way of limiting the number of contacts with spinules due to the topographical roughness. This limited contact regime with contaminants will occur for most particle shapes without projections of the dimensional scale of the wrinkling architecture.

While the adhesion measured on the gecko skin with particles is extremely low, some mechanism must be employed if total removal of the contaminants (e.g. plant matter, bacteria and soil particles) is to take place. There are a number of self-cleaning processes which can potentially clean the gecko skin which include mechanical contortion/motion of the lizard, gravity, wind and water in various forms (e.g. rain, fog and dew). All of these mechanisms will be facilitated if the adhesion of contaminants with the lizard skin is low. Thus, the very low measured adhesion of particulates suggests that removal mechanisms will operate at a high efficiency.

Interestingly, the gecko skin is most likely multifunctional in nature, and thus the unique topographical low adhesion micro- and nano-structure found on the gecko surface demonstrates design characteristics and features for new surfaces where other design attributes (e.g. highly flexible, thin membrane) are also required.

Ethics. This work was conducted under Ethics Approval A1676, and QNP permit WITK05209908.

Competing interests. We declare we have no competing interests.

Funding. We received no funding for this study.

Acknowledgements. The authors thank Sverre Myhra for his assistance with XPS analysis. The authors acknowledge the facilities of the Microscopy and Microanalysis Research Facility at the Centre for Microscopy and Microanalysis at the University of Queensland.

## References

1. Chen P-Y, McKittrick J, Meyers MA. 2012 Biological materials: functional adaptations and bioinspired designs. *Prog. Mater. Sci.* **57**, 1492–1704. (doi:10.1016/j.pmatsci.2012.03.001)
2. Koch K, Barthlott W. 2009 Superhydrophobic and superhydrophilic plant surfaces: an inspiration for biomimetic materials. *Phil. Trans. R. Soc. A* **367**, 1487–1509. (doi:10.1098/rsta.2009.0022)
3. Xu J, Guo Z. 2013 Biomimetic photonic materials with tunable structural colors. *J. Colloid Interface Sci.* **406**, 1–17. (doi:10.1016/j.jcis.2013.05.028)
4. Darmanin T, Guittard F. 2014 Recent advances in the potential applications of bioinspired superhydrophobic materials. *J. Mater. Chem. A* **2**, 16 319–16 359. (doi:10.1039/C4TA02071E)
5. Wisdom KM, Watson JA, Qu X, Liu F, Watson GS, Chen CH. 2013 Self-cleaning of superhydrophobic surfaces by self-propelled jumping condensate. *Proc. Natl Acad. Sci. USA* **110**, 7992–7997. (doi:10.1073/pnas.1210770110)
6. Barthlott W, Neinhuis C. 1997 Purity of the sacred lotus, or escape from contamination in biological surfaces. *Planta* **202**, 1–8. (doi:10.1007/s004250050096)
7. Watson GS, Gellender M, Watson JA. 2014 Self-propulsion of dew drops on Lotus leaves: a potential mechanism for self-cleaning. *Biofouling* **208**, 1170–1174. (doi:10.1080/08927014.2014.880885)
8. Hu HM, Watson JA, Cribb BW, Watson GS. 2011 Fouling of nanostructured insect cuticle: adhesion of natural and artificial contaminants. *Biofouling* **27**, 1125–1137. (doi:10.1080/08927014.2011.637187)
9. Watson GS, Cribb BW, Watson JA. 2010 The role of micro/nano channel structuring in repelling water on cuticle arrays of the lacewing. *J. Struct. Biol.* **171**, 44–51. (doi:10.1016/j.jsb.2010.03.008)
10. Hu HM, Watson GS, Cribb BW, Watson JA. 2011 Non wetting wings and legs of the cranefly aided by fine structures of the cuticle. *J. Exp. Biol.* **214**, 915–920. (doi:10.1242/jeb.051128)
11. Watson JA, Cribb BW, Hsuan Ming Hu, Watson GS. 2011 A dual layer hair array of the brown lacewing: repelling water at different length scales. *Biophys. J.* **100**, 1149–1155. (doi:10.1016/j.bpj.2010.12.3736)
12. Hansen WR, Autumn K. 2005 Evidence for self-cleaning in gecko setae. *Proc. Natl Acad. Sci. USA* **102**, 385–389. (doi:10.1073/pnas.0408304102)
13. Hu S, Lopez S, Niewiarowski PH, Xia Z. 2012 Dynamic self-cleaning in gecko setae via digital hyperextension. *J. R. Soc. Interface* **9**, 2781–2790. (doi:10.1098/rsif.2012.0108)
14. Russell AP. 2002 Integrative functional morphology of the Gekkotan adhesive system (Reptilla: Gekkota). *Integr. Comp. Biol.* **42**, 1154–1163. (doi:10.1093/icb/42.6.1154)
15. Stark AY, Badge I, Wucinich NA, Sullivan TW, Niewiarowski PH, Dhinojwala A. 2013 Surface wettability plays a significant role in gecko adhesion

underwater. *Proc. Natl Acad. Sci. USA* **110**, 6340–6345. (doi:10.1073/pnas.1219317110)

16. Huber G, Mantz GH, Spolenak R, Mecke K, Jacobs K, Gorb S, Arzt NE. 2005 Evidence for capillarity contributions to gecko adhesion from single spatula nanomechanical measurements. *Proc. Natl Acad. Sci. USA* **102**, 16 293–16 296. (doi:10.1073/pnas.0506328102)
17. Huber G, Gorb SN, Hosoda N, Spolenak R, Arzt E. 2007 Influence of surface roughness on gecko adhesion. *Acta Biomater.* **3**, 607–610. (doi:10.1016/j.actbio.2007.01.007)
18. Autumn K *et al*. 2002 Evidence for van der Waals adhesion in gecko setae. *Proc. Natl Acad. Sci. USA* **99**, 12 252–12 256. (doi:10.1073/pnas.192252799)
19. Sun W, Neuzil P, Kustandi TS, Oh S, Samper VD. 2005 The nature of the gecko lizard adhesive force. *Biophys. J.* **89**, L14–L17. (doi:10.1529/biophysj.105.065268)
20. Spinner M, Gorb SN, Westhoff G. 2013 Diversity of functional microornamentation in slithering geckos *Lialis* (Pygopodidae). *Proc. R. Soc. B* **280**, 20132160. (doi:10.1098/rspb.2013.2160)
21. Paré JA, Sigler L, Rosenthal KL, Mader DR. 2006 Microbiology: fungal and bacterial diseases of reptiles. In *Reptile medicine and surgery* (ed. DR Mader), pp. 217–238, 2nd edn. St Louis, MI: Saunders Elsevier.
22. Cresti M, Linskens HE. 2000 Pollen-allergy as an ecological phenomenon: a review. *Plant Biosyst.* **134**, 341–352. (doi:10.1080/11263500012331350495)
23. Smith JL, Lee K. 2003 Soil as a source of dust and implications for human health. *Adv. Agronomy* **80**, 1–32. (doi:10.1016/S0065-2113(03)80001-9)
24. Cariñanos P, Alcázar P, Galán C, Navarro R, Domínguez E. 2004 Aerobiology as a tool to help in episodes of occupational allergy in work places. *J. Invest. Allergol. Clin. Immunol.* **14**, 300–308.
25. Knaapen AM, Borm PJA, Albrecht C, Schins PF. 2004 Inhaled particles and lung cancer. Part A: mechanisms. *Int. J. Cancer* **109**, 799–809. (doi:10.1002/ijc.11708)
26. D'Amato G. 2002 Environmental urban factors (air pollution and allergens) and the rising trends in allergic respiratory diseases. *Allergy* **57**, 30–33. (doi:10.1034/j.1398-9995.57.s72.5.x)
27. Burney PGJ, Newson RB, Burrows MS, Wheeler DM. 2008 The effects of allergens in outdoor air on both atopic and nonatopic subjects with airway disease. *Allergy* **63**, 542–546. (doi:10.1111/j.1398-9995.2007.01596.x)
28. Watson GS, Dinte BP, Blach-Watson JA, Myhra S. 2004 Friction measurements using force versus distance friction loops in force microscopy. *Appl. Surf. Sci.* **235**, 38–42. (doi:10.1016/j.apsusc.2004.05.130)
29. Wilson S. 2005 *A field guide to the reptiles of Queensland*. Sydney, Australia: New Holland.
30. Dalla Valle L, Nardi A, Toffolo V, Niero C, Toni M, Alibardi L. 2007 Cloning and characterization of scale β-keratins in the differentiating epidermis of geckoes show they are glycine–proline–serine-rich proteins with a central motif homologous to avian keratins. *Dev. Dyn.* **236**, 374–388. (doi:10.1002/dvdy.21022)
31. Toni M, Dalla Valle L, Alibardi L. 2007 The epidermis of scales in gecko lizards contains multiple forms of β-keratins including basic glycine–proline–serinerich proteins. J. Proteome Res. **6**, 1792–1805. (doi:10.1021/pr060626+)
32. Ruibal R. 1968 The ultrastructure of the surface of lizard scales. *Copeia* **4**, 698–703. (doi:10.2307/1441836)
33. Rosenberg HI, Russell AP, Cavey MJ. 1992 Development of the subdigital adhesive pads of *Ptyodactylus guttatus* (Reptilia: Gekkonidae). *J. Morphol.* **211**, 243–258. (doi:10.1002/jmor.1052110302)
34. Bauer AM. 1998 Morphology of adhesive tail tips of carphodactyline geckos (Reptilia: Diplodactylidae). *J. Morphol.* **235**, 41–58. (doi:10.1002/(SICI)1097-4687(199801)235:1,41::AID-JMOR4.3.0.CO;2-R)
35. Peattie AM. 2008 Subdigital setae of narrow-toed geckos, including a Eublepharid (Aeluroscalabotes felinus). *Anat. Rec.* **291**, 869–875. (doi:10.1002/ar.20706)
36. Hiller UN. 2009 Water repellence in gecko skin: how do geckos keep clean? In *Functional surfaces in biology, little structures with big effects*, vol. 1 (ed. SN Gorb), pp. 47–53. Dordrecht, The Netherlands: Springer.
37. Thio BJR, Lee J-H, Meredith JC. 2009 Characterization of ragweed pollen adhesion to polyamides and polystyrene using atomic force microscopy. *Environ. Sci. Technol.* **43**, 4308–4313. (doi:10.1021/es803422s)
38. Watson GS, Blach JA, Cahill C, Nicolau DV, Pham DK, Wright J, Myhra S. 2004 Interactions of poly(amino acids) in aqueous solution with charged model surfaces—analysis by colloidal probe. *Biosens. Bioelectron.* **19**, 1355–1362. (doi:10.1016/j.bios.2003.12.017)
39. Watson GS, Myhra S, Cribb BW, Watson JA. 2008 Putative function(s) and functional efficiency of ordered cuticular nano-arrays on insect wings. *Biophys. J.* **94**, 3352–3360. (doi:10.1529/biophysj.107.109348)
40. Israelachvili JN. 1992 *Intermolecular and surface forces*. London, UK: Academic Press.
41. Johnson KL, Kendall K, Roberts AD. 1973 Surface energy and the contact of elastic solids. *Proc. R. Soc. Lond. A* **324**, 310–313. (doi:10.1098/rspa.1971.0141)
42. Huber G, Gorb S, Spolenak R, Arzt E. 2005 Resolving the nanoscale adhesion of individual gecko spatulae by Atomic Force Microscopy. *Biol. Lett.* **1**, 2–4. (doi:10.1098/rsbl.2004.0254)
43. Burton Z, Bhushan B. 2006 Surface characgterization and adhesion and friction properties of hydrophobic leaf surfaces. *Ultramicroscopy* **106**, 709–719. (doi:10.1016/j.ultramic.2005.10.007)
44. Bhushan B, Jung YC, Niemietz A, Koch K. 2009 Lotus-like biomimetic hierarchiacal structures developed by the self-assembly of tubular plant waxes. *Langmuir* **25**, 1659–1666. (doi:10.1021/la802491k)
45. Bhushan B, Jung YC, Koch K. 2009 Micro-, nano- and hierarchical structures for superhydrophobicity, self-cleaning and low adhesion. *Phil. Trans. R. Soc. A* **367**, 1631–1672. (doi:10.1098/rsta.2009.0014)
46. Ma J, Sun Y, Gleichauf K, Lou J, Li Q. 2011 Nanostructure on taro leaves resists fouling by colloids and bacteria under submerged conditions. *Langmuir* **27**, 10 035–10 040. (doi:10.1021/la2010024)
47. Burton Z, Bhushan B. 2005 Hydrophobicity, adhesion, and friction properties of nanopatterned polymers and scale dependence for micro- and nanoelectromechanical systems. *Nano Lett.* **5**, 1607–1613. (doi:10.1021/nl050861b)
48. Blach JA, Watson GS, Busfield WK, Myhra S. 2001 Photo-oxidative degradation in polyisoprene: surface characterization and analysis by atomic force microscopy. *Polym. Int.* **51**, 12–20. (doi:10.1002/pi.780)
49. Watson GS, Schwarzkopf L, Cribb BW, Myhra S, Gellender M, Watson JA. 2015 Removal mechanisms of dew via self-propulsion off the gecko skin. *J. R. Soc. Interface* **12**, 20141396. (doi:10.1098/rsif.2014.1396)